ACS APPLIED MATERIALS & INTERFACES

Research Article

www.acsami.org

Comparing Electron Recombination via Interfacial Modifications in Dye-Sensitized Solar Cells

Luping Li,[†] Shikai Chen,[†] Cheng Xu,[†,‡] Yang Zhao,[†] Nicholas G. Rudawski,[§] and Kirk J. Ziegler*[,†,‡]

[†]Department of Chemical Engineering, University of Florida, Gainesville, Florida 32611, United States

[‡]Department of Materials Science & Engineering, University of Florida, Gainesville, Florida 32611, United States

[§]Major Analytical Instrumentation Center, University of Florida, Gainesville, Florida 32611, United States

Supporting Information

ABSTRACT: Establishing a blocking layer between the interfaces of the photoanode is an effective approach to improve the performance of dye-sensitized solar cells (DSSCs). In this work, HfO_2 blocking layers are deposited via atomic layer deposition (ALD) onto tin-doped indium oxide (ITO) and TiO_2. In both cases, addition of the blocking layer increases cell efficiencies to greater than 7%. The improved performance for a HfO_2 layer inserted between the ITO/TiO_2 interface is associated with an energy barrier that reduces electron recombination. HfO_2 blocking layers between the TiO_2/dye interface show more complex behavior and are more sensitive to the number of ALD cycles. For thin blocking layers on TiO_2, the improved device performance is attributed to the passivation of surface states in TiO_2. A distinct transition in dark current and electron lifetime are observed after 4 ALD cycles. These changes to performance indicate thick HfO_2 layers on TiO_2 formed an energy barrier that significantly hinders cell performance.

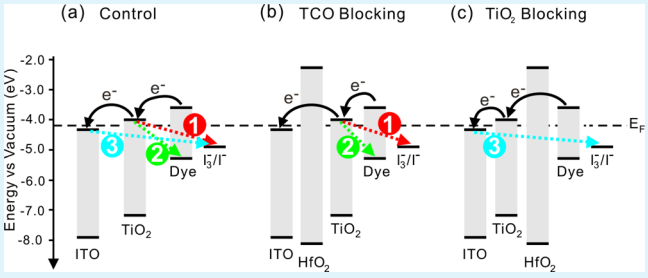

KEYWORDS: *dye-sensitized solar cell, blocking layer, trap states, atomic layer deposition, electron recombination*

INTRODUCTION

Dye-sensitized solar cells (DSSCs) boast low manufacturing cost, ease of fabrication, and good adaptability to various substrates. Among the different types of solar cells, DSSCs are unique since electron transport, light absorption, and hole transport are each handled by different materials in the cell.[1] DSSCs have the potential to replace conventional Si-based solar cells, especially in low-light situations.[2] Enhancing cell efficiency is critical for the advancement of DSSC technology since their conversion is currently relatively low compared to other types of solar cells.

A DSSC is an electrochemical cell that typically consists of a mesoporous TiO_2 nanoparticle layer coated with a photoactive dye on a transparent conductive oxide (TCO) substrate as the photoanode, a platinized TCO as the counter electrode, and a liquid I^-/I_3^- redox couple as the electrolyte. The efficiency of the cell is largely determined by the injection of electrons and their transport through the photoanode. The operation of the DSSC requires that the TCO, TiO_2 nanoparticles, dye molecules, and the I^-/I_3^- redox couple all be in direct contact with each other. This direct contact facilitates fast electron injection from the dye to the TiO_2 and then subsequently to the TCO upon illumination. While intimate contact is needed between all components, the back-reaction of photogenerated electrons at each of these interfaces can also occur.[1,3] These back reactions or electron recombination processes limit the performance of DSSCs.[3−5] Therefore, engineering and controlling these interfaces are critical to the development of efficient DSSCs.

Several approaches have been explored to reduce these recombination processes. Nanowire-based photoanodes in DSSCs have been reported to enhance charge transport due to the presence of a radial electrical field within the nanowires.[6] This radial electrical field helps to draw electrons away from the surface, thereby, reducing electron recombination processes.[7,8] Other studies have focused on modifying the electrolyte solution. Song et al.[9] added cyclodextrins to the electrolyte to form complexes with the triiodide ions that reduced electron recombination and increased DSSC efficiencies. Research has also shown that establishing a dense and compact blocking layer between interfaces of the photoanode can suppress electron recombination. Ceramics with high band gaps, such as HfO_2,[10,11] Al_2O_3,[2,12,13] SiO_2,[10,13] Nb_2O_5,[14] MgO,[15] and ZrO_2,[13,16] have been used as the blocking layer. TiO_2 blocking layers established by sol−gel methods (e.g., $TiCl_4$ treatment) are also effective in improving cell efficiencies.[17,18] However, coatings formed by sol−gel method are often porous and nonuniform in thickness, which greatly reduces their effectiveness and reliability.[12] Atomic layer deposition (ALD) circumvents the drawbacks of sol−gel processing and is able to

Received: August 25, 2014
Accepted: November 20, 2014
Published: November 20, 2014

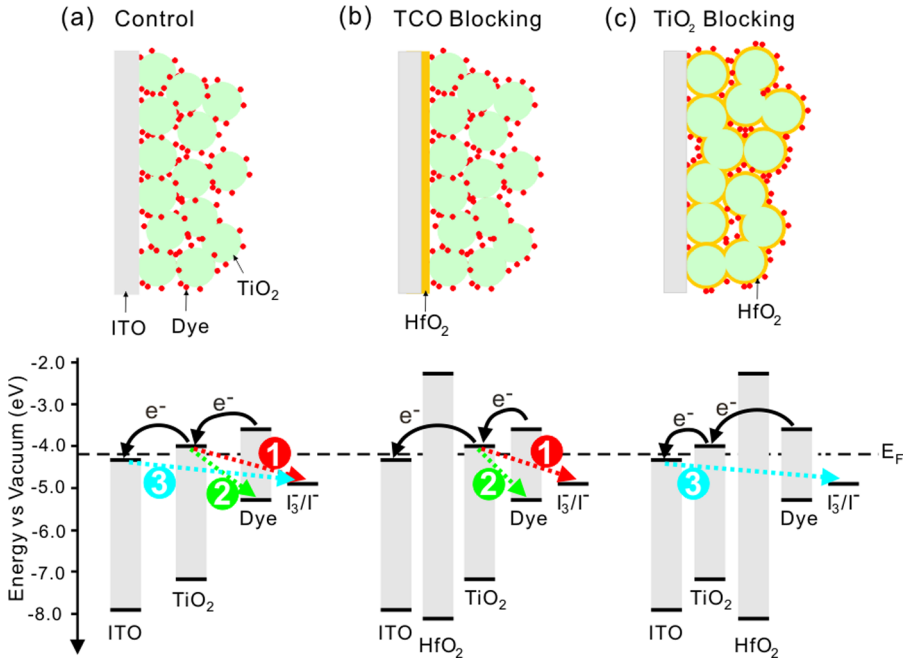

Figure 1. Top panel: Schematic of the three types of photoanodes fabricated. (a) Control consisting of TiO_2 nanoparticles on ITO; (b) TCO blocking layer consisting of HfO_2 deposited on ITO; and (c) TiO_2 blocking layer consisting of HfO_2 deposited on TiO_2 nanoparticles. Bottom panel: The band diagram for each photoanode indicating possible electron recombination processes, such as (1) TiO_2/electrolyte; (2) TiO_2/dye; and (3) ITO/electrolyte.

deposit conformal coatings with high compactness.[19] The self-terminating nature of ALD processes results in accurate control over coating thickness, which is important to the operation of DSSCs.

Depending on the photoanode interface where the blocking layer is inserted, a variety of recombination processes could potentially be suppressed. Inserting a blocking layer between the TCO and TiO_2 interface is expected to suppress electron recombination from the TCO to the electrolyte.[14] A blocking layer between the TiO_2 and dye interface is likely to suppress electron recombination from both the TiO_2 to the dye and TiO_2 to the electrolyte.[10,11] The successfulness of these blocking layers on the performance of DSSCs has ranged from minor improvements to significant increases. For instance, by inserting blocking layers between the TiO_2/dye interface, Lin et al.[12] increased efficiency from 5.75% to 6.50% while Li et al.[16] increased efficiency from 0.27% to 1.08%. By inserting blocking layers between the TCO/TiO_2 interface, Xia et al.[14] increased efficiency from 3.5% to 4.5%.

While these studies consistently show improvement in cell efficiency, the mechanism for suppression of electron recombination at the interfaces often varies by material and deposition method. For instance, some researchers suggest that the effectiveness of these approaches is due to an energy barrier established by the wide band gap of the blocking layer that prevents the back flow of injected electrons.[11,14] On the other hand, dangling bonds and vacancies at the TiO_2 surface induce surface states that have lower energy levels than the conduction band edge in TiO_2.[10,20] Therefore, other studies claim that the passivation of TiO_2 surface states from the blocking layer results in the reduction of electron recombination.[2,16] While many believe that any insulating blocking layer will be effective, it is becoming clear that the conduction band position, surface charge, and electrolyte have a role.[21]

To understand the respective role of blocking layers during DSSC operation, electron recombination on both interfaces (TCO/TiO_2 and TiO_2/dye) should be compared on the same device. This work focuses on how photovoltaic properties of DSSCs are influenced by the inclusion of HfO_2 layers on different interfaces of the photoanode. By inserting the blocking layer at different interfaces and keeping all other fabrication procedures identical, an understanding of how these layers help suppress electron recombination can be achieved. HfO_2 is used as the blocking layer material since it has a large band gap (5.8 eV).[22] Up to 6 cycles of HfO_2 are applied by ALD onto either the TCO or TiO_2 surface. DSSC devices are fabricated, and the photovoltaic properties are evaluated and compared. Open-circuit voltage decay (OCVD) measurements are used to further understand electron recombination processes when HfO_2 blocking layers are deposited onto TiO_2 nanoparticles.

EXPERIMENTAL SECTION

Fabricating Photoanodes. ITO on glass (purchased from Thin Film Devices Inc., US) was used as the TCO substrate. The substrate was cleaned consecutively in water, ethanol, and acetone using ultrasonication. TiO_2 paste (18NR-T, Dyesol Limited, Australia) was applied onto ITO by "doctor blading" and annealed at 520 °C for 10 min. Figure S1 shows a typical cross-sectional SEM image of the TiO_2 film on ITO. The thickness of each TiO_2 film was inspected by SEM after annealing, and only the ones with a thickness of 12 ± 1 μm were used for device fabrication. Figure S1 also shows that the nanoparticles are crystalline with diameters of approximately 20−30 nm. Three types of photoanodes were fabricated: (a) control consisting of TiO_2 nanoparticles on ITO; (b) TCO blocking layer consisting of HfO_2 deposited on ITO; and (c) TiO_2 blocking layer consisting of HfO_2 deposited on TiO_2 nanoparticles. To fabricate the TCO blocking layer photoanode, HfO_2 was first deposited onto a clean ITO substrate by ALD and the TiO_2 layer was subsequently deposited using the doctor blade method described above. To prepare the TiO_2 blocking layer photoanode, the TiO_2 layer was first deposited onto a clean ITO substrate and annealed, followed by HfO_2 deposition by ALD. All

ALD was performed on a Cambridge Nano Fiji 200 system at 175 °C with tetrakis(dimethylamido)hafnium and H_2O as the Hf and O source, respectively. The nominal thickness of each ALD cycle deposit is ~0.11 nm. HfO_2 deposition is not expected to affect the porosity of the TiO_2 film since HfO_2 layers are thin and the measured dye loading was the same before and after HfO_2 deposition (see Figure S5). X-ray photoelectron spectroscopy (XPS) analysis confirmed the deposition of HfO_2 (see Figure S2). A comparison of cell performance between HfO_2 deposited on TiO_2 nanoparticles with and without additional annealing at 520 °C for 10 min showed no difference in performance (not shown). This result suggests that the additional annealing step experienced by the HfO_2 layer deposited on ITO during the annealing of TiO_2 nanoparticles was not a factor.

Preparing DSSC Device. The prepared photoanodes were dyed in N719 (Dyesol) ethanol solution (concentration 3 mM) for ~12 h. The counter electrode solution (CELS, Dyesol) was applied onto cleaned ITO by spin coating and then annealed at 430 °C for 10 min to achieve a thin Pt film. Scotch tape was used as the spacer between the electrodes and the electrolyte was purchased from Dyesol (EL-HPE). The two electrodes were held together by clips during device testing. For each type of photoanode studied, 3–4 devices were tested by illumination through a black aperture with an area of 0.08 cm^2. Pierce's criterion was used to evaluate device performance statistics.

Characterization. The cells were tested under simulated global AM 1.5 spectrum (XPS 200 coupled with 16S, Solar Light Company, US) with a power density of 100 $mW{\cdot}cm^{-2}$. The light source was calibrated with a Si reference cell (RCSi65, PV Measurements, US) before data collection. The J–V curves and OCVD measurements were recorded by a potentiostat (VersaSTAT 3, Princeton Applied Research, US). A two-terminal setup was used where working/sensing electrodes were connected as one terminal and reference/counter electrodes were connected as another terminal. During OCVD measurements, cells were illuminated for a few seconds and the light source was subsequently turned off. OCVD provides useful information on electron-transfer kinetics by monitoring the transient of open-circuit voltage (V_{oc}) during the relaxation from the illuminated quasi-equilibrium state to the dark equilibrium. The electron lifetime (τ_n) was calculated from the slope of the decay curve,[23] $\tau_n = (-k_BT/e)(dV_{oc}/dt)^{-1}$, where k_B is the Boltzmann constant, T is the absolute temperature, and e is the positive elementary charge. An FEI XL40 SEM was used to examine the morphology of the nanoparticle TiO_2 layer. TEM characterization was performed on a JEOL 2010F TEM. A PerkinElmer 5100 XPS system was used to perform compositional analysis.

RESULTS AND DISCUSSION

Although the importance of studying the electron recombination losses of TCO substrates has been emphasized,[24,25] most research has focused on depositing high band gap materials on the TiO_2 nanoparticles[10−12,15] rather than the TCO substrate.[3,14] In this study, HfO_2 blocking layers were deposited on both the TiO_2 nanoparticles and the TCO substrate by ALD. DSSC devices were fabricated from each photoanode and changes to the performance characteristics were determined.

Figure 1 illustrates the three types of photoanodes prepared: (a) control consisting of TiO_2 nanoparticles on ITO without ALD of HfO_2; (b) TCO blocking layer consisting of HfO_2 deposited on ITO; and (c) TiO_2 blocking layer consisting of HfO_2 deposited on TiO_2 nanoparticles. The corresponding band diagram for each type of photoanode is adapted from Bills et al.[3] and Lin et al.[12] and shown below each type of photoanode in Figure 1. Without blocking layers, the three most significant electron recombination processes that hinder performance are the loss of electrons from (1) TiO_2 to electrolyte; (2) TiO_2 to dye; and (3) ITO to electrolyte, as shown in the band diagram of Figure 1a. A HfO_2 blocking layer on ITO is likely to suppress recombination process (3), as shown in the band diagram of Figure 1b. On the other hand, a HfO_2 blocking layer on TiO_2 nanoparticles is expected to suppress recombination processes (1) and (2), as shown in the band diagram of Figure 1c. The effect of the blocking-layer location on the photovoltaic properties are evaluated and compared below.

HfO_2 Blocking Layer on ITO. Figure 2 shows the current–voltage response of devices fabricated with different ALD cycles

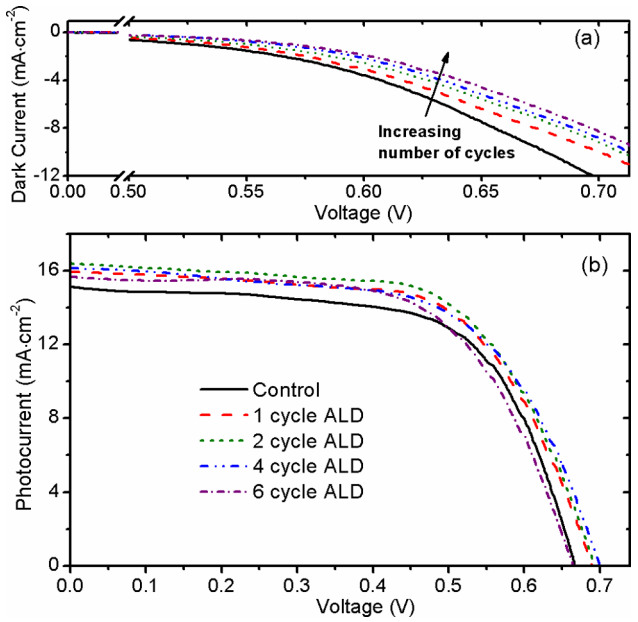

Figure 2. Current–voltage response of cells with different thicknesses (ALD cycles) of a HfO_2 blocking layer on ITO (a) in the dark and (b) under AM 1.5 illumination.

(thicknesses) of HfO_2 on the TCO substrate. The photovoltaic properties for these devices are summarized in Table 1. Figure

Table 1. Photovoltaic Properties of Cells with HfO_2 Blocking Layers on ITO[a]

	V_{oc} [V]	J_{sc} [$mA{\cdot}cm^{-2}$]	FF [%]	η [%]
Control	0.66 ± 0.02	15.01 ± 0.06	65.0 ± 0.6	6.45 ± 0.03
1 Cycle on ITO	0.69 ± 0.02	15.91 ± 0.07	63.0 ± 0.7	6.88 ± 0.04
2 Cycle on ITO	0.68 ± 0.02	16.38 ± 0.08	63.5 ± 0.7	7.09 ± 0.03
4 Cycle on ITO	0.70 ± 0.02	16.09 ± 0.05	60.8 ± 0.5	6.83 ± 0.05
6 Cycle on ITO	0.66 ± 0.01	15.73 ± 0.05	62.9 ± 0.8	6.51 ± 0.05

[a]Average values and standard deviations are based on 3–4 devices.

2a shows the variation of dark current with different ALD cycles. The magnitude of the dark current decreases monotonically with the number of ALD cycles. The smaller dark current is because of the suppressing effect of the blocking layers as the large band gap of HfO_2 creates an energy barrier that retards electron flow from ITO to the electrolyte. The suppression of this electron recombination process from ITO to the electrolyte is likely to increase V_{oc} under illumination. Indeed, Table 1 shows that V_{oc} increases with the number of ALD cycles for up to 4 ALD cycles. The increase of V_{oc} with blocking layer

deposition on TCO is in agreement with earlier work where thin layers of Nb_2O_5 were applied onto FTO.[14]

Without a HfO_2 blocking layer, the control cell has an efficiency (η) of 6.45% under illumination (see Figure 2a and Table 1). Because of the improvements to both V_{oc} and short-circuit current (J_{sc}), the efficiency increased with a single ALD cycle. The enhanced cell efficiency indicates that the electron recombination from the ITO to the electrolyte has been suppressed, as illustrated in Figure 1b. Cell performance was not impacted adversely from the blocking layer since the electrons are able to tunnel through the blocking layers during electron transport from TiO_2 to ITO as long as the blocking layers are thin enough (a few angstroms thick).[19] Indeed, both the series and shunt resistance remained relatively constant, indicating that HfO_2 deposition up to 2 ALD cycles did not have a significant impact on the internal resistance (see Supporting Information) or the fill factor (FF) of the cells. Improved performance occurs for HfO_2 deposition up to 2 ALD cycles, resulting in an efficiency of 7.09% that corresponds to a 10% efficiency enhancement above the control photoanode. However, both η and J_{sc} start to decrease slightly when additional ALD cycles are used. The decreased performance is attributed to the resistive effect of thick HfO_2 since the tunneling probability of electrons falls off exponentially with coating thickness.[19]

HfO_2 Blocking Layer on TiO_2 Nanoparticles. Figure 3 shows the current–voltage response of cells with different ALD

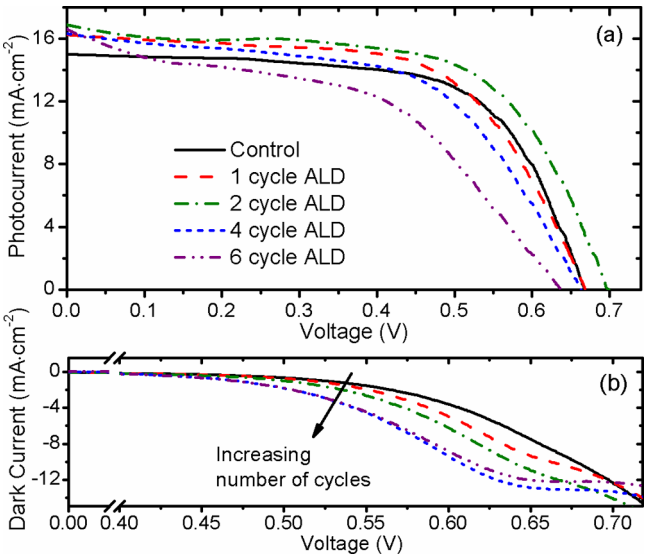

Figure 3. Current–voltage response of cells with different thicknesses (ALD cycles) of a HfO_2 blocking layer on TiO_2 (a) under AM 1.5 illumination and (b) under dark conditions.

cycles of HfO_2 on TiO_2. In comparison to the HfO_2 blocking layer on ITO, the current–voltage response of the HfO_2 blocking layer on TiO_2 in Figure 3a showed more variability in the shape of the curve. The photovoltaic properties for these cells are summarized in Table 2. It is seen that both V_{oc} and J_{sc} increase with the number of ALD cycles for up to 2 cycles. The V_{oc} is determined by the energy difference between the Fermi level of TiO_2 and the I^-/I_3^- redox couple.[1] With blocking layers on TiO_2, the suppressed electron recombination results in higher electron density within the conduction band of TiO_2, which leads to a rise of the Fermi level and, consequently,

Table 2. Photovoltaic Properties of Cells with HfO_2 Blocking Layers on TiO_2[a]

	V_{oc} [V]	J_{sc} [mA·cm^{-2}]	FF [%]	η [%]
Control	0.66 ± 0.02	15.01 ± 0.06	65.0 ± 0.6	6.45 ± 0.03
1 Cycle on TiO_2	0.67 ± 0.02	16.36 ± 0.07	61.0 ± 0.6	6.65 ± 0.03
2 Cycle on TiO_2	0.70 ± 0.01	16.91 ± 0.08	61.6 ± 0.7	7.25 ± 0.04
4 Cycle on TiO_2	0.66 ± 0.01	16.35 ± 0.5	56.4 ± 0.7	6.10 ± 0.05
6 Cycle on TiO_2	0.63 ± 0.02	16.60 ± 0.07	46.8 ± 0.5	4.95 ± 0.03

[a]Average values and standard deviations are based on 3–4 devices.

higher V_{oc}. Shanmugam et al.[10] and Ganapathy et al.[26] also reported increases to V_{oc} when blocking layers are inserted. While Ramasamy et al.[11] saw significant increases in dye loading for dip-coated HfO_2 blocking layers, the increase of J_{sc} seen in Table 2 is not due to changes in dye loading (see Supporting Information) but could be attributed to the increase of electron density in the conduction band of TiO_2.[13] These increases to V_{oc} and J_{sc} for 2 ALD cycles or less occur without significant increases to the series resistance (see Supporting Information). Although the shunt resistance decreases even for a single ALD cycle, the improvements to V_{oc} and J_{sc} yield higher conversion efficiencies. For these reasons, a HfO_2 blocking layer on TiO_2 with 2 cycles of ALD produced the best performing cell of the study with a cell efficiency of 7.25%, corresponding to an efficiency enhancement of 10.4%.

While the HfO_2 blocking layer on TiO_2 is beneficial up to 2 ALD cycles, the enhancement degrades quickly and becomes detrimental to performance if additional cycles are used. After 2 ALD cycles, the series resistance starts increasing dramatically and significantly impacts the performance of the cell (see Supporting Information). Most notably, the higher series and lower shunt resistance cause the fill factor to fall substantially. The degradation of the resistances within the cell leads to a rapid fall in efficiency as more than 2 ALD cycles are used. Figure 3b also shows dramatic changes to the dark current–voltage response of cells as the thickness of a HfO_2 blocking layer on TiO_2 increases. Similar to the deposition of Nb_2O_5,[21] the magnitude of the dark current increases with thicker blocking layers of HfO_2. Interestingly, there is an inflection in the dark current at ~0.625 V for 4 and 6 ALD. For these thicker blocking layers, the dark current is suppressed at higher potentials.

The dramatic changes in both photocurrent and dark current performance at different ALD cycles suggest that competing effects are occurring within the cell as the number of cycles increase. To better understand the processes that are occurring within these devices as the HfO_2 blocking layer on TiO_2 becomes thicker, open-circuit voltage decay (OCVD) measurements were conducted. These transient measurements help illustrate how electron recombination processes proceed under dark conditions. Figure 4a shows that more ALD cycles result in slower voltage decay, indicating slower electron recombination. The decay measurements once again show that there is a unique change to the operation of the cell once 4 ALD cycles coat the TiO_2 layer. Analysis of the decay measurements in Figure 4b indeed show that a longer electron lifetime (τ_n) is observed for increased ALD cycles. At a constant voltage of 0.5 V, Figure 4c shows that τ_n in the DSSCs initially increases linearly with up to 4 ALD cycles. However, τ_n deviated

dx.doi.org/10.1021/am505742y | ACS Appl. Mater. Interfaces 2014, 6, 20978–20984

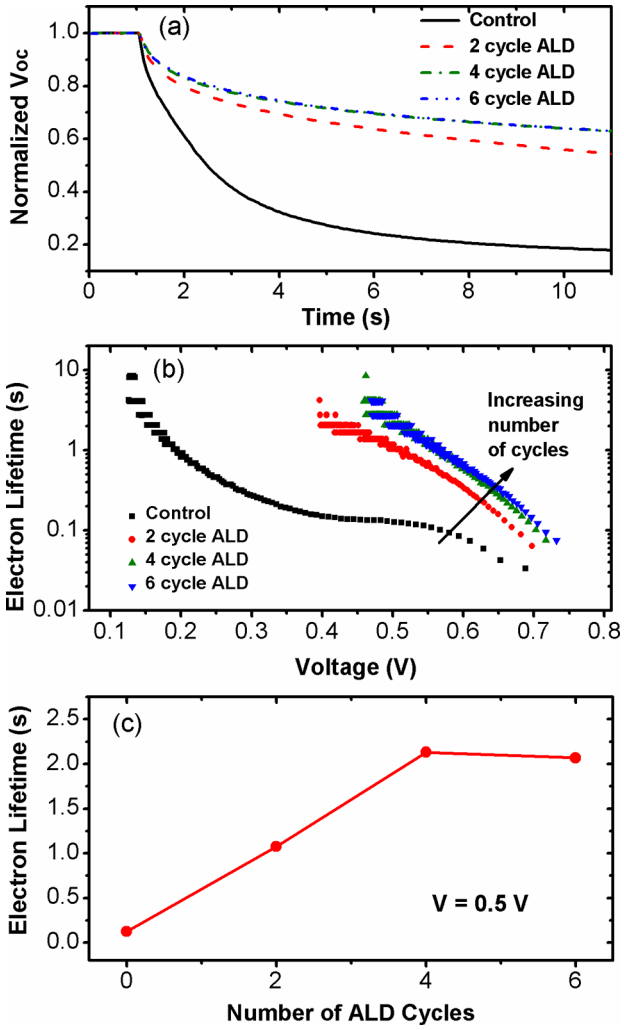

Figure 4. (a) Normalized open-circuit voltage decay (OCVD) of DSSCs when different cycles of HfO_2 are deposited onto TiO_2. Note that decay curves for 4 and 6 ALD cycles overlap. (b) Calculated electron lifetime for the DSSC with different ALD cycles. (c) Dependence of electron lifetime at a constant voltage of 0.5 V on the number of ALD cycles of HfO_2. Line is drawn for visual aid.

dramatically from the linear increase after 6 ALD cycles and plateaued.

Without a HfO_2 blocking layer, the TiO_2 is in direct contact with both dye molecules and electrolyte. As Figure 1a illustrated, electron loss from the TiO_2 nanoparticles can occur by recombination with either the electrolyte or the dye. While both processes are possible, the recombination with the electrolyte (process 1) typically dominates since the regeneration of the oxidized dye by the electrolyte is much faster than the recombination of electrons with oxidized dye.[20] If surface states exist in TiO_2, then electron recombination can also occur with the electrolyte through these surface states. Therefore, electron transport to the electrolyte can occur from either the conduction band (1a) or from the trap states (1b) in the TiO_2 layer under dark conditions, as shown in Figure 5a. In addition, electrons are exchanged between the conduction band and trap states (1c). Figure 5b shows the expected effect on dark current if the HfO_2 blocking layer acts as an energy barrier. In this situation, both pathway 1a and 1b are hindered by the energy barrier. The reduced flow of electrons would ultimately lead to lower dark current than the control sample. Indeed, decreased dark current is routinely reported for blocking layers[11,26,27] and is analogous to the HfO_2 layer on ITO described above. If the blocking layer passivates some of the surface states of the TiO_2, the magnitude of the dark current is expected to increase. This electron loss is because the surface (trap) states immobilize electrons and slow down electron transport.[28,29] Therefore, passivating these surface states results in higher dark current, as shown in Figure 5c. The increase in magnitude of dark current with the number of ALD cycles on TiO_2 (Figure 3b) indicates that initial HfO_2 depositions (up to 4 ALD cycles) passivated surface states in TiO_2. Continued deposition of HfO_2 (6 ALD cycles) leads to a decrease in the dark current, suggesting thick HfO_2 blocking layers form an energy barrier that eventually hinders pathway 1a. Once this energy barrier is formed, a dramatic decrease in cell efficiency is seen for thick blocking layers (Table 2).

It is important to note that the longer electron lifetimes observed in Figure 4 would not necessarily be expected for a device that has higher dark current. However, an important difference is that OCVD measurements are illuminated.

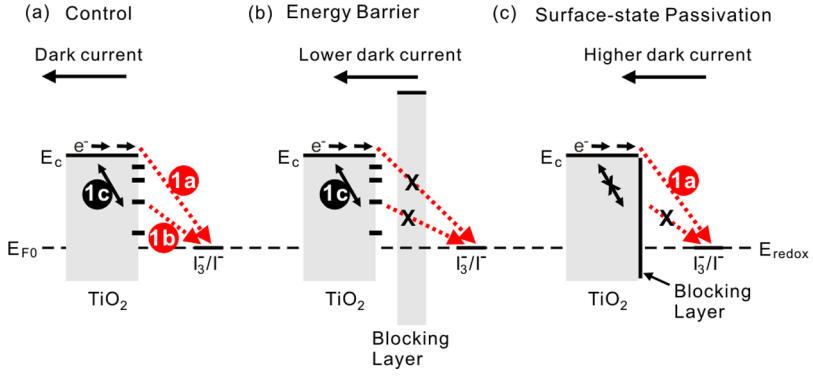

Figure 5. Band diagrams illustrating electron recombination processes occurring under dark conditions from (a) control consisting of TiO_2 nanoparticles on ITO and for a blocking layer deposited on TiO_2 nanoparticles if the blocking layer acts as either (b) an energy barrier or (c) a surface-state passivation layer. E_{F0} is the position of the Fermi level at the dark, which equilibrates with the redox potential E_{redox} in the electrolyte, and E_C is the conduction band energy. Possible electron pathways for dark current include recombination from either (1a) the TiO_2 conduction band or (1b) the TiO_2 surface states to the electrolyte as well as (1c) electron exchange between the conduction band and surface states. Lower dark current is expected in (b) since the energy barrier hinders electron transport, while higher dark current is expected in (c) since surface states that slow down electron transport are passivated.

Bisquert et al.[28] showed that the electron lifetime should be a function of the surface states as well as the internal temperature of the DSSC. They have suggested that heating of the device during illumination can explain such inversions at certain distributions of trap states at the surface and bulk. If the energy of the surface states is above the Fermi level, the resistance decreases resulting in higher dark current. As the temperature increases from illumination, the Fermi level is raised toward the conduction band. Once the Fermi level is above the energy of the surface states, the trapping rate decreases. This change to the trapping rate increases the resistance, resulting in longer electron lifetimes under illumination.

CONCLUSIONS

Although inserting blocking layers between the interfaces of a photoanode have been shown to improve the performance in DSSCs, the respective role of blocking layers during DSSC operation has not been compared on the same device to understand the differences in electron recombination at the TCO or TiO_2 interface. In this work, HfO_2 blocking layers are inserted between the ITO/TiO_2 and TiO_2/electrolyte interfaces. Although both blocking layers improved the performance of the cell, the mechanism is different at each interface. HfO_2 deposited onto ITO acted as an energy barrier layer that suppressed electron recombination from ITO to the electrolyte. The energy barrier was effective at reducing electron recombination as long as the thickness of the blocking layer was 2 ALD cycles or smaller. At thicknesses above 2 ALD cycles, the decreased tunneling probability hindered performance. When HfO_2 was deposited onto TiO_2, two distinct regions were observed. For thin blocking layers, the HfO_2 passivated the surface states of TiO_2 and resulted in longer electron lifetimes. However, thicker blocking layers formed an energy barrier that significantly degraded performance. The improved cell performance characteristics yielded a maximum efficiency of 7.09% and 7.25% for 2 ALD cycles of HfO_2 onto ITO and TiO_2, respectively.

ASSOCIATED CONTENT

Supporting Information

SEM and TEM images of TiO_2 nanoparticles, internal resistances of DSSCs, UV−vis spectroscopy, and X-ray photoelectron spectroscopy data. This material is available free of charge via the Internet at http://pubs.acs.org.

AUTHOR INFORMATION

Corresponding Author

*E-mail: kziegler@che.ufl.edu.

Funding

This work was funded by the National Science Foundation (CBET-1033736).

Notes

The authors declare no competing financial interest.

ACKNOWLEDGMENTS

The authors acknowledge the support of the Donors of the American Chemical Society Petroleum Research Fund, the University of Florida Opportunity Fund, and the National Science Foundation (CBET-1033736) for support of this research.

REFERENCES

(1) Hardin, B. E.; Snaith, H. J.; McGehee, M. D. The Renaissance of Dye-Sensitized Solar Cells. *Nat. Photonics* **2012**, *6*, 162−169.

(2) Prasittichai, C.; Hupp, J. T. Surface Modification of SnO_2 Photoelectrodes in Dye-Sensitized Solar Cells: Significant Improvements in Photovoltage Via Al_2O_3 Atomic Layer Deposition. *J. Phys. Chem. Lett.* **2010**, *1*, 1611−1615.

(3) Bills, B.; Shanmugam, M.; Baroughi, M. F. Effects of Atomic Layer Deposited HfO_2 Compact Layer on the Performance of Dye-Sensitized Solar Cells. *Thin Solid Films* **2011**, *519*, 7803−7808.

(4) Ma, W.; Jiao, Y.; Meng, S. Modeling Charge Recombination in Dye-Sensitized Solar Cells Using First-Principles Electron Dynamics: Effects of Structural Modification. *Phys. Chem. Chem. Phys.* **2013**, *15*, 17187−17194.

(5) Ma, W.; Jiao, Y.; Meng, S. Predicting Energy Conversion Efficiency of Dye Solar Cells from First Principles. *J. Phys. Chem. C* **2014**, *118*, 16447−16457.

(6) Law, M.; Greene, L. E.; Johnson, J. C.; Saykally, R.; Yang, P. D. Nanowire Dye-Sensitized Solar Cells. *Nat. Mater.* **2005**, *4*, 455−459.

(7) Hill, J. J.; Haller, K.; Wangyao, G.; Banks, N.; Ziegler, K. J. Conductive Nanowires Coated with a Semiconductive Shell as the Photoanode in Dye-Sensitised Solar Cells. *Int. J. Nano Biomater.* **2012**, *4*, 196−212.

(8) Hill, J. J.; Banks, N.; Haller, K.; Orazem, M. E.; Ziegler, K. J. An Interfacial and Bulk Charge Transport Model for Dye-Sensitized Solar Cells Based on Photoanodes Consisting of Core−Shell Nanowire Arrays. *J. Am. Chem. Soc.* **2011**, *133*, 18663−18672.

(9) Song, H.-K.; Yoon, J.; Won, J.; Kim, H.; Yeom, M. S. New Approach to the Reduction of Recombination in Dye-Sensitised Solar Cells via Complexation of Oxidised Species. *J. Nanosci. Nanotechnol.* **2013**, *13*, 5136−5141.

(10) Shanmugam, M.; Baroughi, M. F.; Galipeau, D. Effect of Atomic Layer Deposited Ultra Thin HfO_2 and Al_2O_3 Interfacial Layers on the Performance of Dye Sensitized Solar Cells. *Thin Solid Films* **2010**, *518*, 2678−2682.

(11) Ramasamy, P.; Kang, M.-S.; Cha, H.-J.; Kim, J. Highly Efficient Dye-Sensitized Solar Cells Based on HO_2 Modified TiO_2 Electrodes. *Mater. Res. Bull.* **2013**, *48*, 79−83.

(12) Lin, C.; Tsai, F.-Y.; Lee, M.-H.; Lee, C.-H.; Tien, T.-C.; Wang, L.-P.; Tsai, S.-Y. Enhanced Performance of Dye-Sensitized Solar Cells by an Al_2O_3 Charge-Recombination Barrier Formed by Low-Temperature Atomic Layer Deposition. *J. Mater. Chem.* **2009**, *19*, 2999−3003.

(13) Palomares, E.; Clifford, J. N.; Haque, S. A.; Lutz, T.; Durrant, J. R. Control of Charge Recombination Dynamics in Dye Sensitized Solar Cells by the Use of Conformally Deposited Metal Oxide Blocking Layers. *J. Am. Chem. Soc.* **2002**, *125*, 475−482.

(14) Xia, J.; Masaki, N.; Jiang, K.; Yanagida, S. Sputtered Nb_2O_5 as a Novel Blocking Layer at Conducting Glass/TiO_2 Interfaces in Dye-Sensitized Ionic Liquid Solar Cells. *J. Phys. Chem. C* **2007**, *111*, 8092−8097.

(15) Sujuan, W.; Hongwei, H.; Qidong, T.; Jing, Z.; Sheng, X.; Conghua, Z.; Ying, Y.; Hao, H.; BoLei, C.; Bobby, S.; Xing-Zhong, Z. Enhancement in Dye-Sensitized Solar Cells Based on Mgo-Coated TiO_2 Electrodes by Reactive DC Magnetron Sputtering. *Nanotechnology* **2008**, *19*, 215704.

(16) Li, T. C.; Góes, M. r. S.; Fabregat-Santiago, F.; Bisquert, J.; Bueno, P. R.; Prasittichai, C.; Hupp, J. T.; Marks, T. J. Surface Passivation of Nanoporous TiO_2 via Atomic Layer Deposition of ZrO_2 for Solid-State Dye-Sensitized Solar Cell Applications. *J. Phys. Chem. C* **2009**, *113*, 18385−18390.

(17) O'Regan, B. C.; Durrant, J. R.; Sommeling, P. M.; Bakker, N. J. Influence of the $TiCl_4$ Treatment on Nanocrystalline TiO_2 Films in Dye-Sensitized Solar Cells. 2. Charge Density, Band Edge Shifts, and Quantification of Recombination Losses at Short Circuit. *J. Phys. Chem. C* **2007**, *111*, 14001−14010.

(18) Choi, H.; Nahm, C.; Kim, J.; Moon, J.; Nam, S.; Jung, D.-R.; Park, B. The Effect of $TiCl_4$-Treated TiO_2 Compact Layer on the

Performance of Dye-Sensitized Solar Cell. *Curr. Appl. Phys.* **2012**, *12*, 737−741.
(19) Hartman, T. E.; Chivian, J. S. Electron Tunneling through Thin Aluminum Oxide Films. *Phys. Rev.* **1964**, *134*, 1094.
(20) Bisquert, J.; Cahen, D.; Hodes, G.; Rühle, S.; Zaban, A. Physical Chemical Principles of Photovoltaic Conversion with Nanoparticulate, Mesoporous Dye-Sensitized Solar Cells. *J. Phys. Chem. B* **2004**, *108*, 8106−8118.
(21) Chandiran, A. K.; Nazeeruddin, M. K.; Grätzel, M. The Role of Insulating Oxides in Blocking the Charge Carrier Recombination in Dye-Sensitized Solar Cells. *Adv. Funct. Mater.* **2014**, *24*, 1615.
(22) Robertson, J. High Dielectric Constant Oxides. *Eur. Phys. J. Appl. Phys.* **2004**, *28*, 265−91.
(23) Zaban, A.; Greenshtein, M.; Bisquert, J. Determination of the Electron Lifetime in Nanocrystalline Dye Solar Cells by Open-Circuit Voltage Decay Measurements. *ChemPhysChem* **2003**, *4*, 859−864.
(24) Cameron, P. J.; Peter, L. M.; Hore, S. How Important Is the Back Reaction of Electrons Via the Substrate in Dye-Sensitized Nanocrystalline Solar Cells? *J. Phys. Chem. B* **2005**, *109*, 930−936.
(25) Zhang, S.; Yang, X.; Qin, C.; Numata, Y.; Han, L. Interfacial Engineering for Dye-Sensitized Solar Cells. *J. Mater. Chem. A* **2014**, *2*, 5167.
(26) Ganapathy, V.; Karunagaran, B.; Rhee, S.-W. Improved Performance of Dye-Sensitized Solar Cells with TiO_2/Alumina Core−Shell Formation Using Atomic Layer Deposition. *J. Power Sources* **2010**, *195*, 5138−5143.
(27) Kay, A.; Grätzel, M. Dye-Sensitized Core−Shell Nanocrystals: Improved Efficiency of Mesoporous Tin Oxide Electrodes Coated with a Thin Layer of an Insulating Oxide. *Chem. Mater.* **2002**, *14*, 2930−2935.
(28) Bisquert, J.; Fabregat-Santiago, F.; Mora-Seró, I.; Garcia-Belmonte, G.; Giménez, S. Electron Lifetime in Dye-Sensitized Solar Cells: Theory and Interpretation of Measurements. *J. Phys. Chem. C* **2009**, *113*, 17278−17290.
(29) Richter, C.; Schmuttenmaer, C. A. Exciton-Like Trap States Limit Electron Mobility in TiO_2 Nanotubes. *Nat. Nanotechnol.* **2010**, *5*, 769−772.